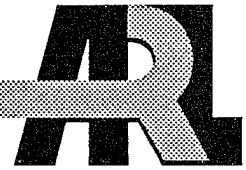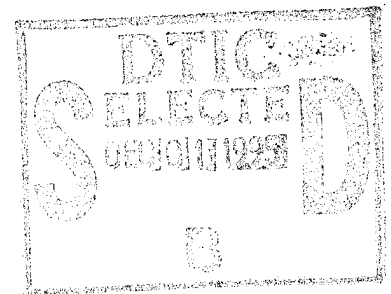ARMY RESEARCH LABORATORY

A Pulse-Forming Network Design for Electrothermal-Chemical (ETC) Combustion Characterization of Solid Propellants

M. Del Guercio
H. Burden
I. Stobie
K. White
G. Katulka
S. Driesen

ARL-MR-261   September 1995

19951130 074

NOTICES

Destroy this report when it is no longer needed. DO NOT return it to the originator.

Additional copies of this report may be obtained from the National Technical Information Service, U.S. Department of Commerce, 5285 Port Royal Road, Springfield, VA 22161.

The findings of this report are not to be construed as an official Department of the Army position, unless so designated by other authorized documents.

The use of trade names or manufacturers' names in this report does not constitute indorsement of any commercial product.

ERRATA RE:
A PULSE-FORMING NETWORK DESIGN FOR ELECTROTHERMAL-CHEMICAL
(ETC) COMBUSTION CHARACTERIZATION OF SOLID PROPELLANTS,
ARL-MR-261, SEPTEMBER 1995

Request the following pen and ink change be made to the above named report:

On Page 14, fourth line from top, change "(Figure 6)" to read "(Figure 9)."

REPORT DOCUMENTATION PAGE

Public reporting burden for this collection of information is estimated to average 1 hour per response, including the time for reviewing instructions, searching existing data sources, gathering and maintaining the data needed, and completing and reviewing the collection of information. Send comments regarding this burden estimate or any other aspect of this collection of information, including suggestions for reducing this burden, to Washington Headquarters Services, Directorate for Information Operations and Reports, 1215 Jefferson Davis Highway, Suite 1204, Arlington, VA 22202-4302, and to the Office of Management and Budget, Paperwork Reduction Project(0704-0188), Washington, DC 20503.

1. AGENCY USE ONLY (Leave blank)	2. REPORT DATE	3. REPORT TYPE AND DATES COVERED
	September 1995	Final, January - October 1994

4. TITLE AND SUBTITLE
A Pulse-Forming Network Design for Electrothermal-Chemical (ETC) Combustion Characterization of Solid Propellants

5. FUNDING NUMBERS

PR: 1L162618AH80

6. AUTHOR(S)
M. Del Guercio, H. Burden, I. Stobie, K. White, G. Katulka, and S. Driesen

7. PERFORMING ORGANIZATION NAME(S) AND ADDRESS(ES)

U.S. Army Research Laboratory
ATTN: AMSRL-WT-PA
Aberdeen Proving Ground, MD 21005-5066

8. PERFORMING ORGANIZATION REPORT NUMBER

ARL-MR-261

9. SPONSORING/MONITORING AGENCY NAMES(S) AND ADDRESS(ES)

10. SPONSORING/MONITORING AGENCY REPORT NUMBER

11. SUPPLEMENTARY NOTES

12a. DISTRIBUTION/AVAILABILITY STATEMENT

Approved for public release; distribution is unlimited.

12b. DISTRIBUTION CODE

13. ABSTRACT (Maximum 200 words)

The combustion of solid propellants subjected to plasma augmentation has been studied with a 300-kJ maximum stored energy Pulse-Forming Network (PFN) in the range of 1 kJ/g of electrical energy over a 1.2-ms pulse length. A closed chamber vessel is used for the combustion of these solid propellants in which the plasma is injected via a plasma generator. Since the need to characterize the effects of plasma augmentation on propellant combustion may require a greater pulse length than the 1.2 ms initially provided by the PFN used at the U.S. Army Research Laboratory (ARL), a PFN upgrade providing a 2.4-ms pulse length with a 400-kJ maximum stored energy was implemented. When operated at 5 to 7% of the maximum stored energy, the PFN provides augmentation in the range of 1 kJ/g of propellant. Calculations, design, and fabrication are detailed. Also discussed are plasma generator modifications dictated by the increase in pulse length and energy input needed for test firings.

14. SUBJECT TERMS			15. NUMBER OF PAGES
plasma generators, combustion chamber gases, metallic erosion, plasma injection			38
			16. PRICE CODE

17. SECURITY CLASSIFICATION OF REPORT	18. SECURITY CLASSIFICATION OF THIS PAGE	19. SECURITY CLASSIFICATION OF ABSTRACT	20. LIMITATION OF ABSTRACT
UNCLASSIFIED	UNCLASSIFIED	UNCLASSIFIED	UL

INTENTIONALLY LEFT BLANK.

ACKNOWLEDGMENTS

iii

INTENTIONALLY LEFT BLANK.

TABLE OF CONTENTS

Intentionally left blank.

LIST OF FIGURES

vii

LIST OF TABLES

viii

1. INTRODUCTION

A closed chamber study investigating the combustion of solid propellants subjected to plasma injection has been conducted at the U.S. Army Research Laboratory (ARL) using a 129.4-cm^3 closed vessel with an electrode assembly that includes a plasma generator and an erosion nozzle (Figure 1). A lumped element transmission line Pulse-Forming Network (PFN) with a 300-kJ maximum energy output (Figure 2a) powered the injector. It provided a pulse length of 1.2 ms and was operated in the range of 20 kJ per 20 g of propellant (1-kJ/g energy density). The need to characterize the effects on propellant combustion due to longer plasma injection duration (2.4 ms) motivated the PFN upgrade to be described. The modifications included the addition of two capacitors and construction of bus work, damping resistors, and eight new inductors. Design and fabrication aspects of the induction coil construction are detailed as well as plasma generator design changes implemented as the firing program progressed.
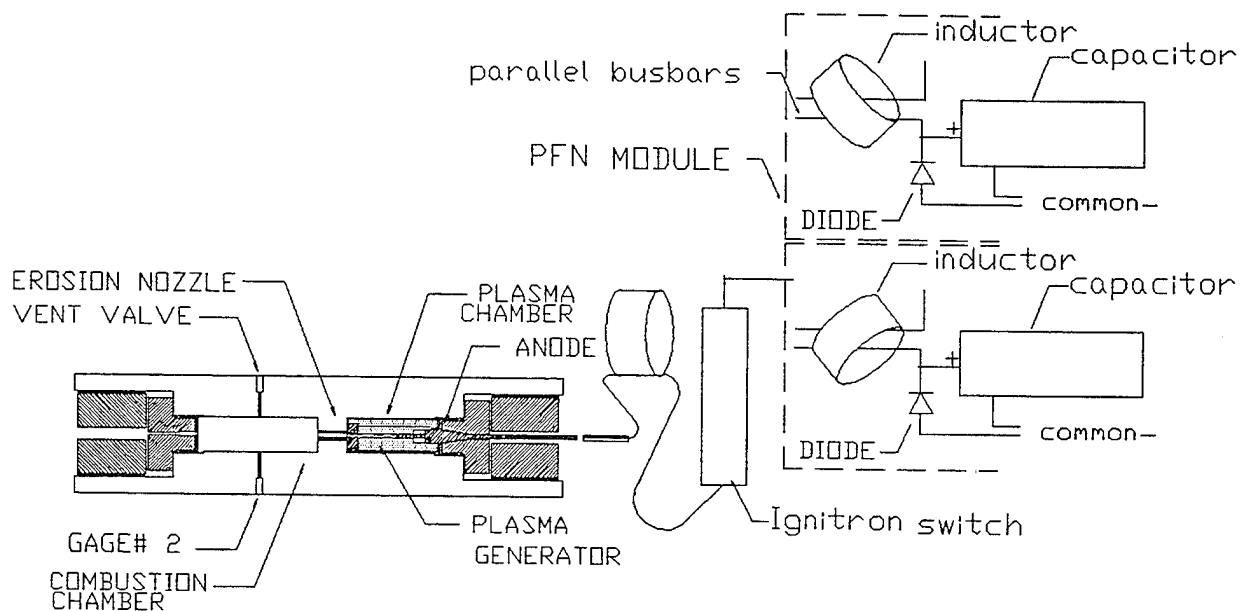
Figure 1. Closed chamber and plasma generator.

1

2. MODIFICATIONS

Through circuit analysis using the code Microcap (Electronic Circuit Analysis Program, property of Spectrum Software, Sunnyvale, CA), it was determined that two more 830-µF capacitors added to the six in use in the original PFN, plus a change to eight 30-µH inductors, would most economically extend the 1.2-ms pulse length to the 2.4 ms desired. This provided an output impedance close to the 100-mΩ value of the load, and so maximizing the power transfer into it.

Figure 2a shows a schematic of the 1.2-ms pulser. The current and voltage profiles (Figure 2b) of the 1.2-ms pulser fired at an initial charging capacitor voltage of 5 kV (corresponding to 60 kJ of stored energy) show the pulse length. Figure 3a shows the schematic of the 2.4 ms PFN; Figures 3b and 3c, the simulated and actual 100-mΩ resistive load tests at 5-kV input voltage; and Figure 3d, the power and energy dissipated at the load for a 2.4-ms pulser firing.

3. DESIGN CRITERIA

The problems faced in this upgrading included installing eight coils in the space formerly occupied by six coils and providing the added support for their increased weight. This had to be done while retaining the design criteria of the earlier design:

(a) arrange adjacent coils' axes at right angles and strive for the greatest separation to minimize mutual coupling, which is difficult to calculate and achieve accurately

(b) maintain the greatest separation between coils and field-sensitive Ignitron and diodes

(c) orient the diodes so that their currents do not interact with the magnetic fields of the parallel plate bus and force nonuniform diode current distributions

(d) orient all coils so that their fields would have the least effect on diodes.

The resistance of the conductors is a function of the depth to which current has penetrated the aluminum and this, in turn, is a function of time. Bennett and Marvin (1962), following an approach by Haines (1959) for continuous, oscillating currents, found an expression for current density vs. depth and time in parallel plates subjected to transient current ramps. They solved Maxwell's form of Ampere's and
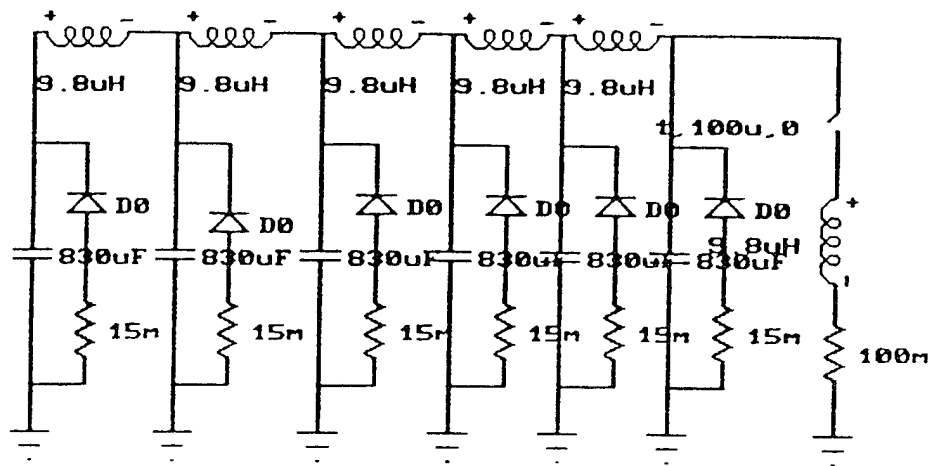
2

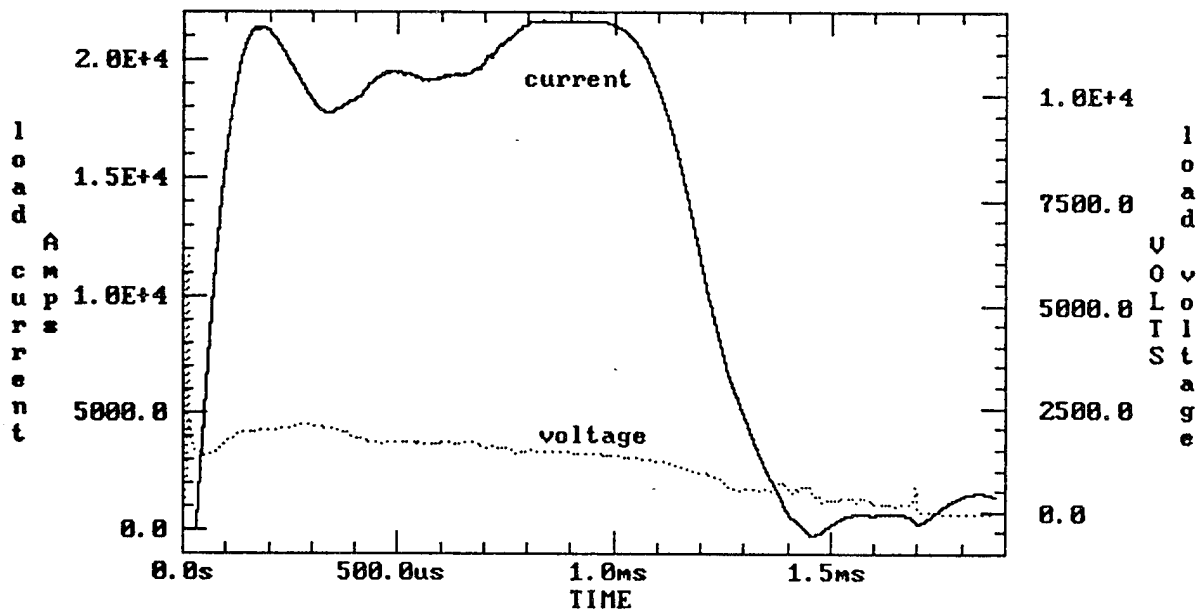Figure 2a. 1.2-ms pulser schematic.

Figure 2b. ETC firing, 5-kV, 1.2-ms pulse.

3
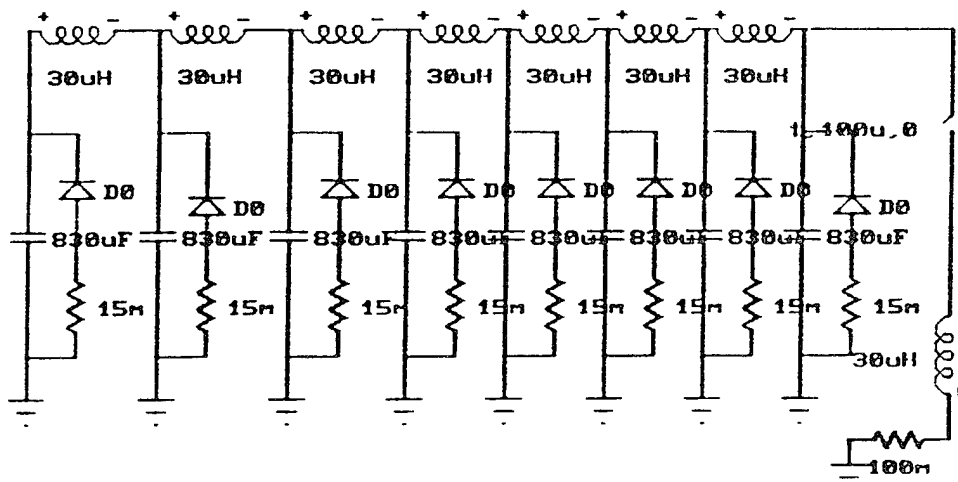
Figure 3a. 2.4-ms pulser schematic.
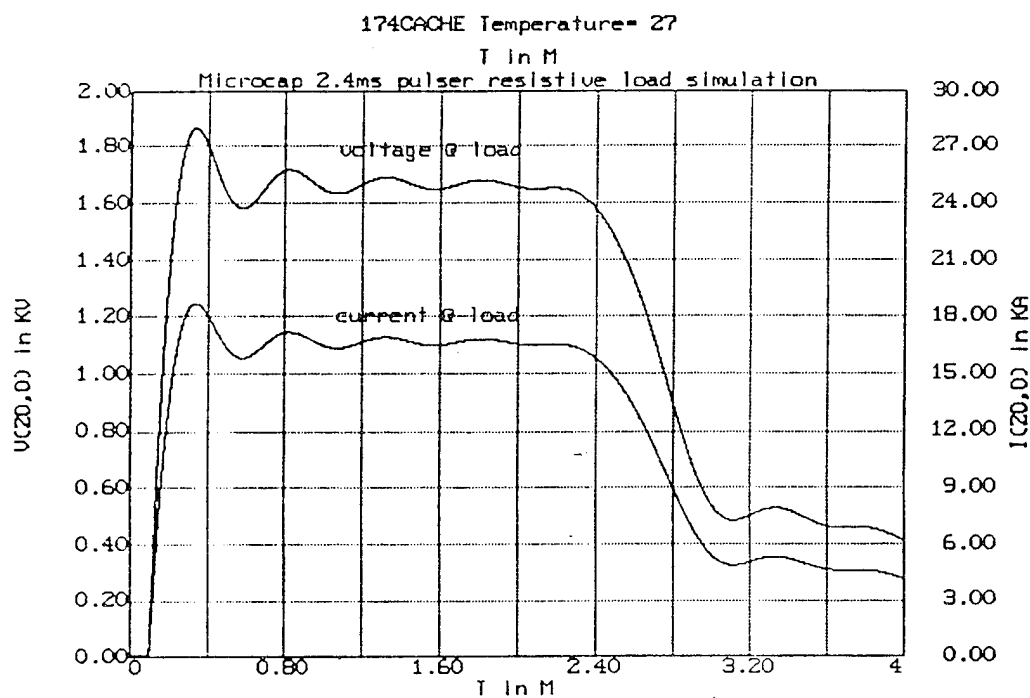
Figure 3b. Microcap simulation.

4
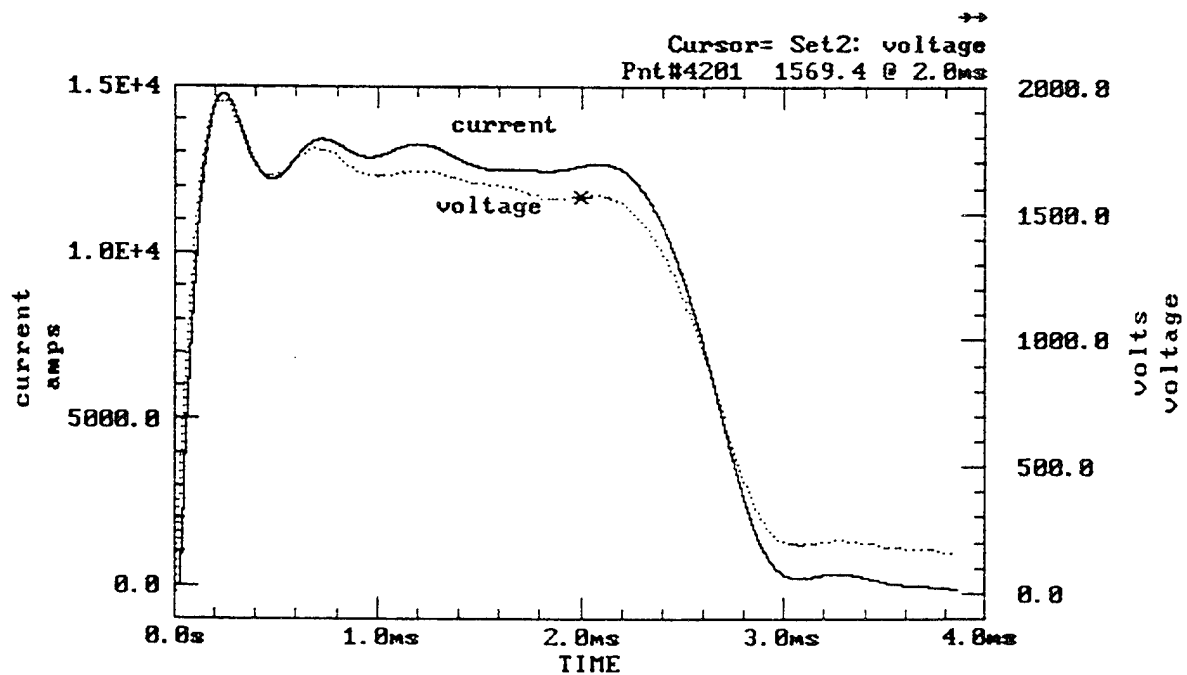
Figure 3c. ETC firing, 5-kV, 2.4-ms pulse.
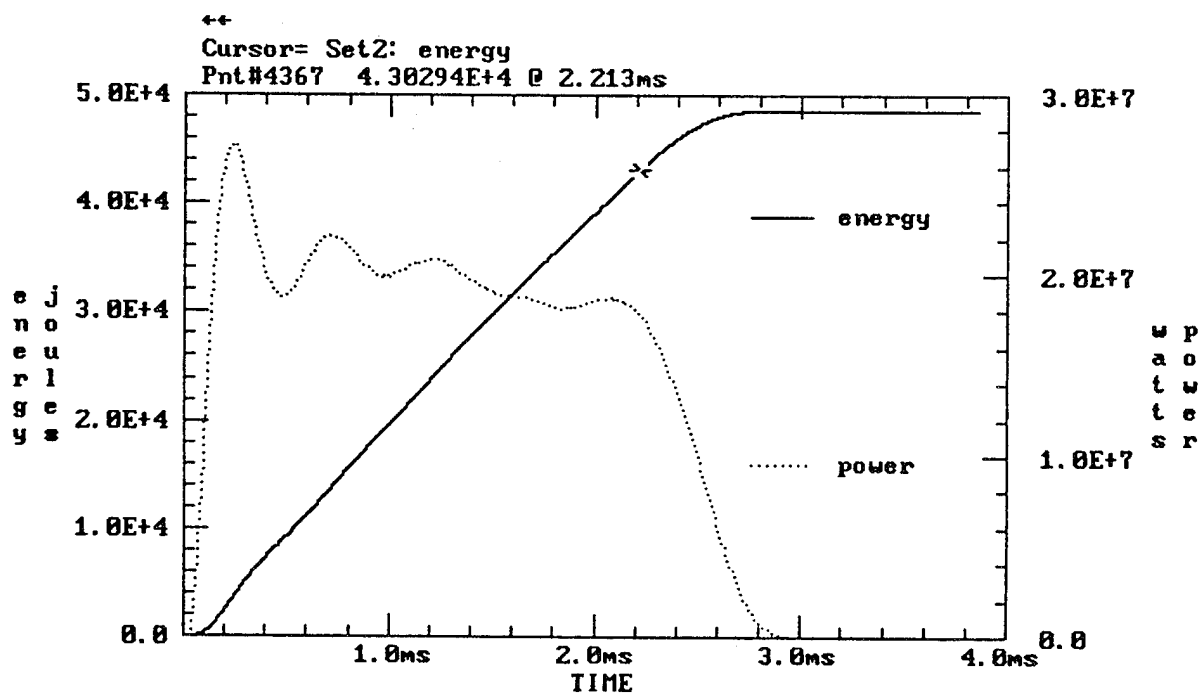
Figure 3d. Power and energy, 2.4-ms pulse.

5

Faraday's laws, coupled by Ohms's law, using the Laplace transform method for dimensionless current density with a linear ramp as the driving function. Such a ramp is a good approximation to a sine function, damped or undamped, during the first 10–15% of a cycle. By squaring their expression for current-density, integrating it over the cross section of a conductor, and dividing by its conductivity, they derived a time-dependant function for power loss in the conductor. They then determined an expression for effective-resistance R by setting this power loss equal to I^2R, I being the ramp's instantaneous total-current through the conductor. The variables were in dimensionless form; x, the dimensionless depth, is given by

$$x = x'/a,$$

(1)

x' being the actual depth and a being the full thickness of the conductor, both in meters. Dimensionless time, y, is given by

$$y = t/\mu\sigma a^2,$$

(2)

μ for nonferrous materials being the value for free space $4\pi E\text{-}07$, σ being the conductivity of the material ($3.7E + 07$ mho/m for aluminum), and t being the actual time. The current density function is then

$$i(x,y) = \frac{\omega}{wa}\left[y + 2\sum_{m=1}^{\infty}\frac{\cos(m\pi x)}{m^2\pi^2}(1 - e^{-m^2\pi^2y})\right].$$

(3)

Note that $\omega = \omega'\mu\sigma a^2$ in which $\omega' = (1/I_p)dI/dt$ (I being the instantaneous and I_p the total peak current in amperes, t the time in seconds, and w the width of the conductor in meters). It should be observed that, if current density were uniform everywhere, the quantity $\omega y/wa$, relative magnitudes of the former to the latter, would be displayed as in Table 1.

The relation for the ratio of transient effective-resistance to DC resistance is:

$$\frac{R(y)}{R_{DC}} = 1 + \frac{2}{\pi^4y^2}\sum_{n=1}^{\infty}\frac{(1 - e^{-n^2\pi^2y})^2}{n^4}.$$

(4)

Table 1. Magnitudes of Calculated-Distribution Current Densities Relative to Those for a Hypothetical/Uniform Distribution (Linear Ramp Driving-Function)

		Dimensionless Times y							
		0.01	0.05	0.12	0.2	0.6	1.0	3.0	5.0
Dimensionless Depths x	0.0	11.15	5.02	3.22	2.51	1.55	1.33	1.11	1.07
	0.2	1.006	2.02	1.86	1.65	1.25	1.15	1.05	1.03
	0.4	0.020	0.62	0.95	1.02	1.02	1.01	1.00	1.00
	0.6	0.001	0.14	0.44	0.61	0.86	0.91	0.97	0.98
	0.8	0.000	0.023	0.19	0.38	0.76	0.85	0.95	0.97
	1.0	0.000	0.005	0.12	0.31	0.72	0.83	0.94	0.97

A tabulation (Table 2) of values for this expression is given. Actual times for a given conductor are found as $t = \mu \sigma a^2 y$; actual depths, $x' = xa$; μ, σ, and a, are all physical constants for the given conductor.

Table 2. Ratios of Transient to DC Resistance vs. Scaled Time Increments

Time, y	$R(y)/R_{DC}$	Time, y	$R(y)/R_{DC}$
0.001	19.705	0.5	1.088
0.002	13.934	1.0	1.022
0.005	8.813	1.2	1.015
0.01	6.232	1.5	1.010
0.02	4.407	2.0	1.006
0.05	2.787	2.2	1.005
0.1	1.972	2.5	1.004
0.2	1.423	—	—

Typical of the bus bars used in the ARL pulser are thickness $a = 0.00635$ m, permeability $\mu = 4\pi\text{E-07}$ H/m, and conductivity $\sigma = 3.7\text{E} + 07$ Ω^{-1} (aluminum); thus, $\mu\sigma a^2 = 1.875\text{E-03}$. The applied pulse reasonably approximates a ramp rising to its peak in 150.0E-06 seconds, or in the dimensionless frame, 0.08; at the peak of the current, the table shows that these bus bars are twice as resistive as for DC.

The bus work from the old unit was utilized in the upgrading. Some bus extensions were added to provide desired positioning of the larger new inductors. All except the final inductor are positioned by means of these parallel plate extensions. The final inductor is located on the load-side of the ignitron switch to get it away from the field-sensitive diode packs and ignitron. Each individual bus bar has the shape of a U lying on its side, its open end away from the capacitor, and connected to it at its middle point. All inductors then are connected in series while the capacitors form the legs of a π configuration (Figure 4).
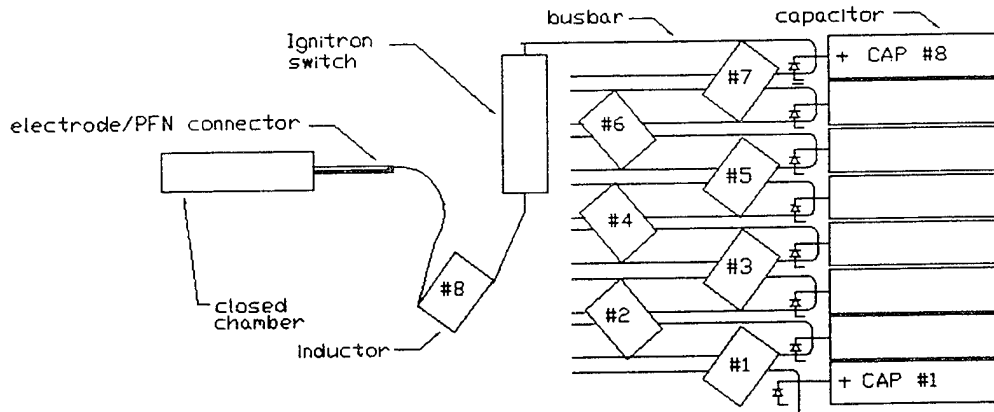
Figure 4.   2.4-ms PFN schematic.

3.1 Calculations. The number of turns required to obtain an inductance L of 30-μH on a 15.3-in-diameter form was determined using the Nagaoka formula (Grover 1982) and its tabulation for the constant K.

$$L = 0.004\pi^2 \, N^2 \, (a^2 \, K/b) \; \mu\text{H,} \tag{5}$$

a being the radius (in centimeters) measured from the center of the coil to the center of the conductor, b the center to center length of the winding (approximate tube length), K a function of the $b/2a$ ratio, and

N the number of turns. A computer program was written that started with an estimate of the number of turns needed. The program determined the winding length required by the insulated wire, then interpolated the table (Grover 1982) to find the corresponding values of K. The formula then produced a new value of N and a new length. The interpolation then found a new K value. This process was repeated iteratively until values of N, b, and K converged to a sufficiently constant and consistent set. It then computed the outside dimensions of the physical space occupied by the coil and the DC resistance of the winding and its corresponding L/R decay time. The program calculated the radial bursting force for a given value of current i. This routine recognized that the expansive force developed by current flow in a coil may be determined by equating the change of electromagnetic energy in the coil to the mechanical work done in expansion $\Delta E = F \Delta a$. The energy stored in a coil is

$$E = (1/2) \, Li^2 \, . \tag{6}$$

Equation 5 relates the coil's inductance to its physical dimensions when an increase in its radius a causes its inductance to increase (as given by the derivative).

$$\Delta L/\Delta a = 0.0395 \, (N^2/b) \, (2aK + a^2 \Delta K/\Delta a) \, . \tag{7}$$

Then the change in energy (for an unchanging current) would be

$$\Delta E/\Delta a = (1/2) \, i^2 \Delta L/\Delta a \, . \tag{8}$$

Since, for a mechanical system,
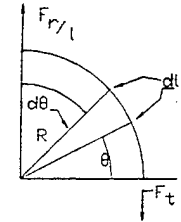
$$\Delta E = F_r \Delta \, , \tag{9}$$

by solving for radial force F_r and substituting from Equation 8, we find

$$F_r = (1/2) \, i^2 \, [0.0395 \, (N^2/b) \, (2aK + a^2 \Delta K/\Delta a)] \, . \tag{10}$$

The computer calculated $\Delta K/\Delta a$ for the tabular interval containing K, and produced an estimate of the radial force distributed over the entire winding. This force distribution was assumed uniform and as a radial force F_r/l per unit length, in analogy with the three-dimensional method of computing hoop, or

9

tangential stress in a pressure vessel. The tangential component of this radial force per length was integrated over the length of a quarter turn of the coil to obtain the tension force F_t in the conductor.

$$F_t = \int_0^{l/4} \frac{F_r}{l}\sin\theta \, dl = \frac{F_r}{l} \int_{\pi/2}^{0} R\sin\theta \, d\theta = \frac{F_r R}{l} . \qquad (11)$$

When this force is divided by the wire cross section, it approximates the tensile stress tending to break the copper winding. This stress should not exceed a safe value for copper. Under normal operating conditions, our design indicated a large margin of safety. However, in the case of catastrophic failures (capacitor breakdown, bus work arcs to ground, arcs across load, etc.), currents may rise to excessive levels, and Kevlar 29 cloth wraps were used to add strength. The effective thickness, T_e, of the no. 352 Clark-Schwebel cloth used was approximated by dividing the published weight per unit area of the cloth by the published density of the Kevlar 29.

$$T_e = (1.767E\text{-}01 \text{ kg/m}^2) \, / \, (1.439E03 \text{ kg/m}^3) = 1.23E\text{-}04 \text{ m} . \qquad (12)$$

The cloth is nominally 0.254-mm thick, so 48% was used as the packing density of the threads. Each turn on the coil occupies 32.8 mm of coil length and, so, is covered by this width of cloth. The urethane potting compound (Hysol XVS-0104) encasing the coil should distribute applied force over the whole area of the Kevlar cloth. The calculated tangential force of 20612 N for a 100-kA discharge produces a stress of 153 MPa in the copper wire and may stretch it. If this force is transferred to the cloth, the stress induced equals force divided by cross section. The cross section is the product of

$$\text{packing density} \times \text{width} \times \text{packing density} \times \text{thickness} \qquad (13)$$

or

$$0.48 \times 3.28E\text{-}02 \text{ m} \times 0.48 \times 2.54E\text{-}4 \text{ m} = 1.92E\text{-}06 \text{ m}^2. \qquad (14)$$

The stress is

$$0.0206 \text{ MN} \, / \, 1.92E\text{-}06 \text{ m}^2 = 10{,}700 \text{ MPa}, \qquad (15)$$

which is three times 3,625 MPa, the maximum stress for Kevlar. Consequently, four layers of cloth were wrapped around the coil prior to potting.

10

3.2 Component Modifications. The requirement that the pulse length, which is proportional to $\sqrt{(LC)}$, be increased, while the line's characteristic impedance, which is proportional to $\sqrt{(L/C)}$, is maintained at its power-maximizing match to the 100-mΩ capillary impedance, dictated the total inductance L and the total capacitance C increase by the same factor. Doubling the size of the six coils to 20 μH and using twice the number of 830-μF capacitors would have worked, however, neither the added six capacitors nor the space for them was available. The aforementioned compromise was selected because its large excess of available energy, in spite of its impedance mismatch, was less critical than the pulse length desired. The eight 30-μH coils and two 830-μF capacitors were used as in Figure 3a. The resulting 2.4-ms pulser's characteristic impedance of 190 mΩ did not match, as expected, the 100-mΩ impedance of the plasma's capillary, but the modified PFN design turned out the desired pulse length with a maximum stored energy of 400 kJ (eight capacitors each rated at 11 kV storing up to 50 kJ). Later resistive tests demonstrated that the pulser's efficiency was in the 70% range, which was the same as the 1.2 ms PFN.

The total capacitance was increased from 4.98 mF (830 μF × 6) to 6.64 mF (830 μF × 8), and the total inductance, from 60 μH (6 × 9.8 μH) to 240 μH (8 × 30 μH). Two additional resistances, in series with the crowbar-diodes which impede voltage reversal in the caps, were manufactured similar to the previous ones, utilizing a Nichrome strip 914 mm × 76 mm in an inductance-lowering zig-zag configuration. These resistors limit the current through the expensive crowbar diodes, and in doing so, protect them from damage should the load become a short circuit. Their impedance value of 15 mΩ was found adequate through a Microcap simulation.

All connecting bus work to and from the inductors was secured at approximately 1-ft intervals by G-11 clamps to counter the magnetic pressure produced by the high currents flowing in and out of the inductors, which tends to separate the bus bars. The limited space within the range constrained the diameter for the new inductors to about 406 mm and the maximum length to 330 mm. Also, as the magnetic flux linkage between adjacent coils had to be minimized to reduce the mutual inductance, a 90° angle was desired between their axes, complicating their placement even further.

3.3 Inductor Fabrication. Each of the eight inductors was wound on a plastic pipe with a 305-mm length, a 389-mm outside diameter (OD), and 11.2-mm-thick walls. A 15.9-mm OD, 20.5-m-long rubber-insulated, 2/0-AWG-copper welding cable was folded in half. Its ends were passed from the inside to the outside of the coil tube through two adjacent holes. The cable ends were then twisted with

a carefully controlled pitch that when wound on the form nested with the twists of the adjacent turns. Winding was done by hand-turning a lathe that was fitted with a dividing head. Commercial Litz wire of the required current capacity has a larger diameter and would have required an unacceptably longer or larger diameter coil. A two-layer coil (possibly of smaller volume) may experience higher stresses and has its start and finish at the same end of the form with resulting insulation demands. The chosen configuration added conductor cross section with acceptable increase in coil length while the crude Litz effect of its twist equalized currents in the parallel conductors.

To counter the expansive magnetic pressure on the windings, as current is pulsed through, they were tightly wrapped with Kevlar cloth and potted in Hysol epoxy which mechanically coupled the coil to the Kevlar in a solid casting. The Hysol consisted of two components mixed to approximately a 400-g A, to 280-g B ratio. To avoid air bubbles and thus improve the tensile and shear properties of the cured epoxy, a vacuum (up to 1.5 mm Hg) was applied to each sample mixture.

3.4 Circuitry. Energy "dumping" to abort the PFN charging process, or in case of a misfire, is controlled through fiber optic links. The load voltage measuring circuit is comprised of a 266-Ω resistor string and a series 100-μF blocking capacitor, which together span the load. In times short with respect to the time constant RC, the current through the resistor is proportional to the load voltage. The lead to the resistor chain is encircled by a Pearson transformer (a Rogowski coil wound on a magnetic core, whose high L/R ratio renders it self-integrating) that senses the current and produces a proportional voltage (in this instance, 0.1 V/A). Additional fiber optics were installed to operate a Ross high-voltage relay used for shorting the 100-μF blocking capacitor used in the voltage measuring circuit at the load, as this capacitor could become fully energized if the load opens. The current measurement at the load is done as on the previous PFN, through a Rogowski coil.

3.5 PFN Testing. The eight modules are triggered simultaneously by one Ignitron closing switch. Solid-state crow-barring protects each capacitor from voltage reversals. Because the pulse profile desired requires only one Ignitron switch, the conditions for diode damage (Figure 5b) are reduced as the simultaneous discharge of the capacitors decreases the chances of large di/dt or high reverse dV/dt across the conducting crow-bar diode (Katulka et al. 1990).
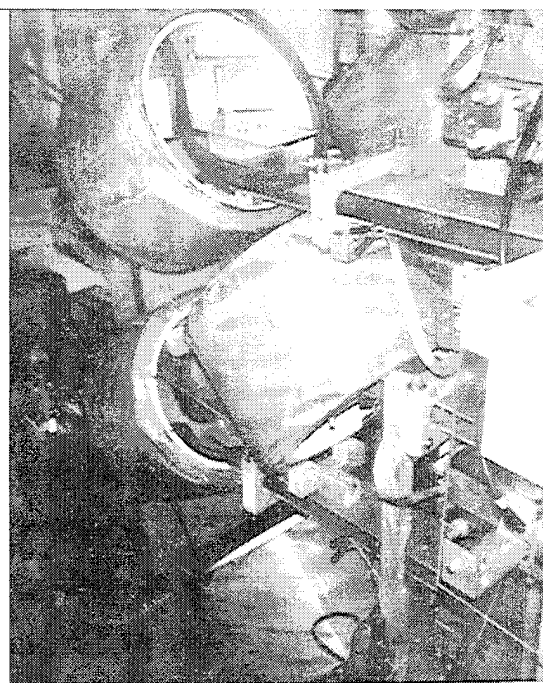
12

Figure 5a. 2.4-ms ARL pulser.

Figure 5b. Bus bars and crowbar diodes.

As the transition from the 1.2-ms pulser to the 2.4-ms pulser was implemented, the resistive dummy load tests at 5-kV input voltage revealed data acquisition noise problems (83-kJ input, 60 kJ at the load) and a short at the PFN/electrode connector. The actual ETC firings (i.e., JA2 propellant ignited by plasma injection), however, revealed bonding occurring on components of the plasma injector to the plasma chamber walls, making disassembly difficult. This bonding caused erosion on the plasma chamber wall, which further complicated the chamber sealing from the propellant combustion gases. What follows is a description of the results found through inspection of the damaged components, and the reasons and theory on which the modifications were based.

3.6 Load Testing. The PFN ETC setup has the electrode-chamber head and E-glass liner-nozzle assembly inserted into the vessel's plasma chamber with the electrode end protruding about an inch through a heavy retaining nut that impedes the chamber head from expulsion (Figure 6). On the previous 1.2-ms pulser (300 kJ), an insulated 102-mm-long copper connector secured to the electrode end and to the PFN output provided the path for the PFN discharge.

The PFN output consisted of a 38.1-mm-OD of solid copper tube threaded in one end to accept the electrode end and welded to the last inductor output wires on the opposite end. During resistive load tests at 3 kV with the 2.4-ms pulser (400 kJ), a short was observed between the flat area of the retaining nut
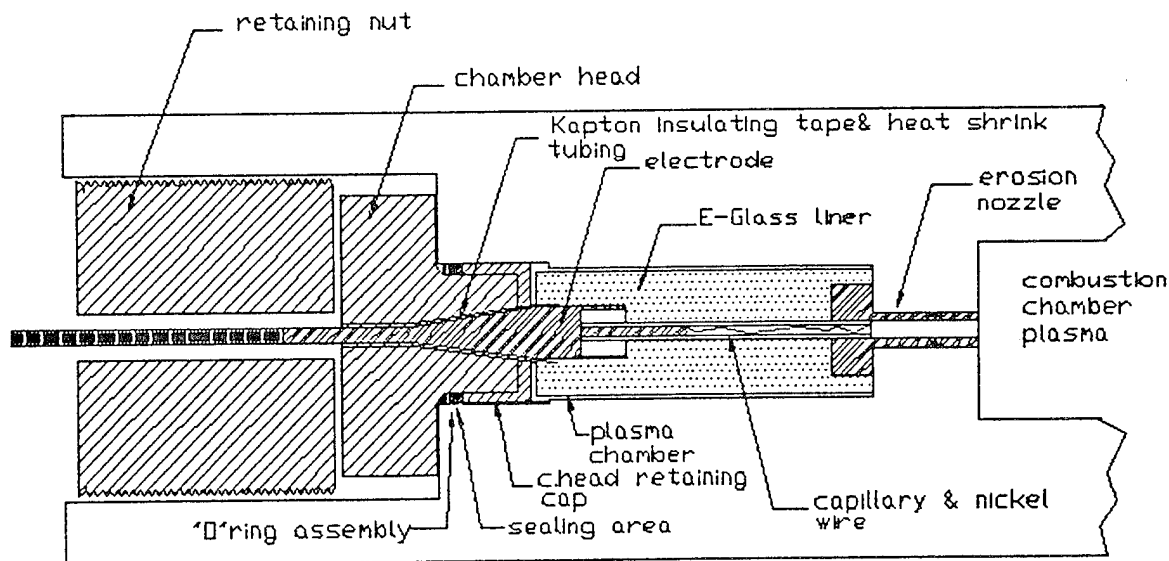
13

Figure 6. Plasma chamber design.

and the exposed frontal area of the copper tube (PFN output). For this reason, several layers of dielectric protected by heat shrinkable tubing, were added around a new 204-mm extended copper connector.

The PFN output copper tube was also insulated in its totality; only the holes for the electrode tightening screws (Figure 6) were left exposed. Measurements made for di/dt and voltage at the load for the 2.4-ms PFN resistive test became unusually noisy at over 3 kV of voltage input. A short occurring at the 3-kV resistive load test between some of the capacitor casings and the bus bars was suspect as the cause for this noise. After Mylar sheets (0.127-mm thick) were inserted in between the casings and the bus bars, the noise was eliminated from di/dt and voltage fiber-optic acquired signals even at higher voltages (5 kV).

4. CLOSED CHAMBER ETC FIRINGS

4.1 First ETC Firing. During the first ETC firing (Table 3), with the plasma generator assembled as shown in Figures 7a and 7b, a short was observed at the chamber head area (Figure 6), which seats the electrode. Also minor damage was observed at the nozzle base O-ring sealing area. JA2 propellant was used because of its high density and energy. This firing had the configuration assembly shown in Figures 7a and 7b using a 0.076-mm-thick nickel wire to connect the electrode (anode) tip to the
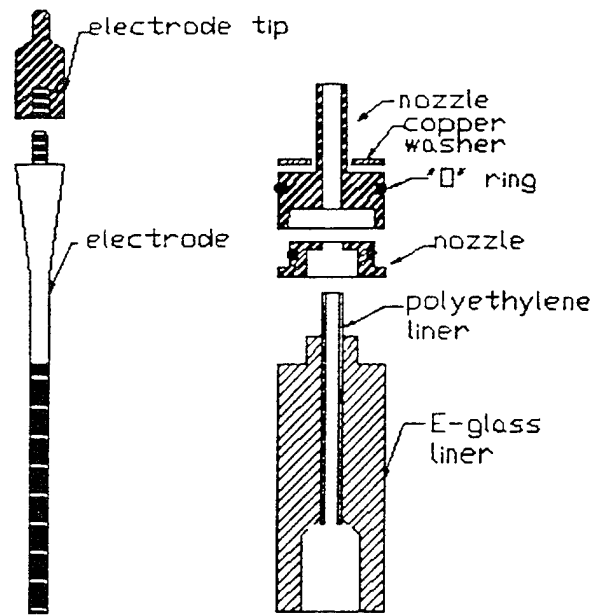
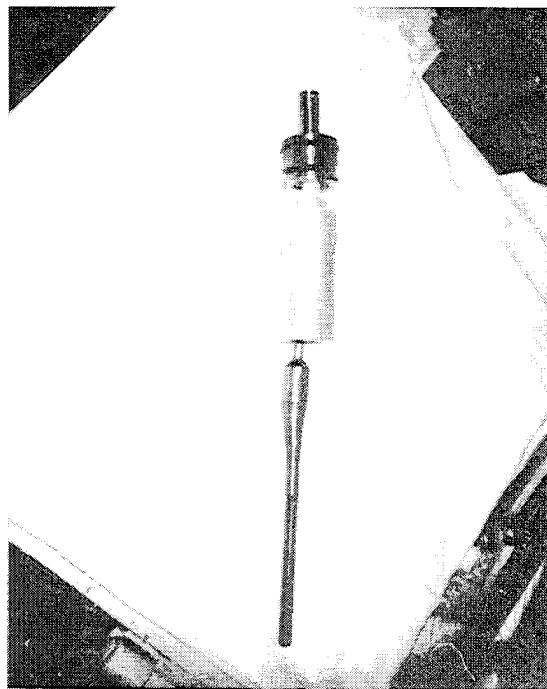Figure 7a. Plasma assembly, model 1, schematic.
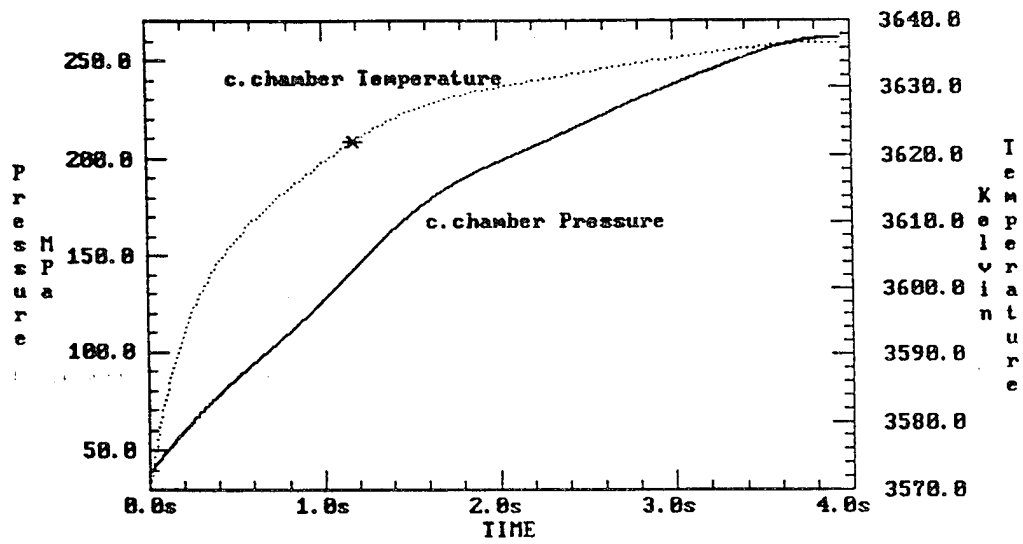

Figure 7b. Model 1, photograph.

Figure 8a. Chamber pressure and temperature vs. time.

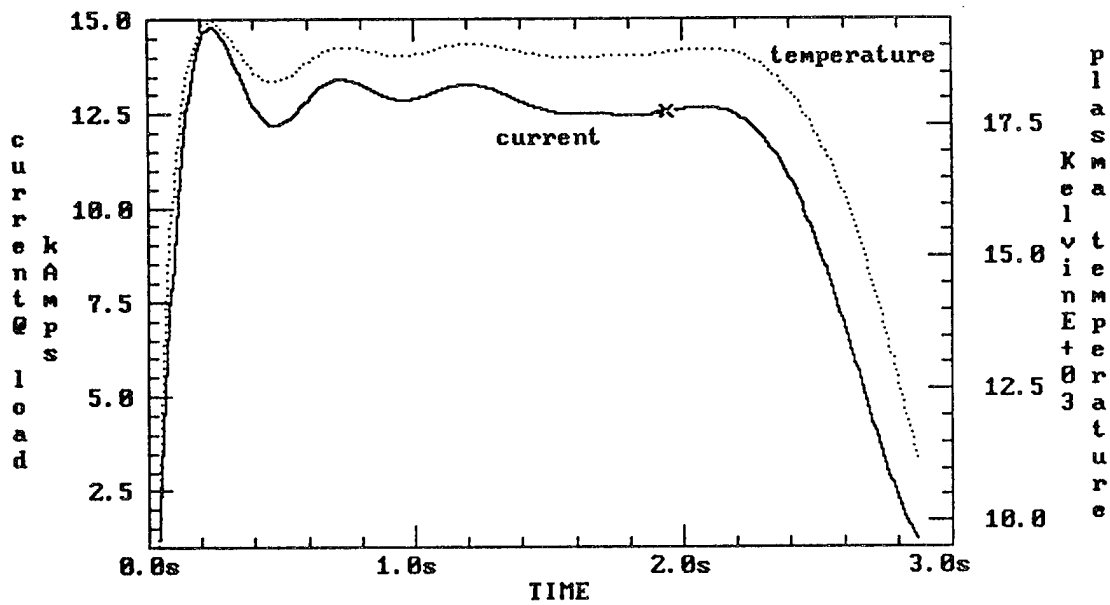Figure 8b. Plasma current and temperature.

16

Table 3. ETC Firings With 2.4-ms Pulser

Date	Test	Input Voltage (kV)	Configuration
07/05/94	First shot	5	Figure 8a and 8b, model 1
07/06/94	Second shot	5	Figure 8a and 8b, model 1
08/31/94	Third shot	5	Figure 10, model 2
09/16/94	Fourth shot	5	Figures 14 and 15, model 3

grounding nozzle (cathode). Hot combustion gases and/or plasma were suspected of melting the Kapton insulating tape and heat-shrink tubing. This is true, since all the electrode components are high-pot tested to well above the system voltage prior to ETC firings. Voltage and di/dt data indicate that the shorts occurred between 2 and 2.4 ms.

The pressure and temperature of the plasma (Phuong 1994), as well as for the combustion gases for JA2 (Oberle 1994), were estimated using the BRLCB (Oberle 1993) code. It was concluded at that time that the short was caused solely by the plasma heat. The combustion chamber reaches 3,000 K between 2 and 3 ms (Figure 8a), while the plasma reaches temperatures of 20,000 K (Phuong 1994) in the same time frame (Figure 8b). The suspected plasma traveled downwards through the erosion nozzle channel, the polyethylene liner, and around the electrode tip (which presses the thin [0.102 mm] nickel wire against the insulating E-glass liner [Figure 9]), down to the insulation area where the conical section of the electrode presses against the chamber head, causing a short. For the previous 5-kV, 1.2-ms pulse, this time was sufficient for such insulation to hold the electrode voltage during the plasma discharge. Closed chamber pressure and temperature, as well as plasma temperature and load current, are shown in Figures 8a and 8b, respectively.

4.2 Second ETC Firing. Major metallic deposits were observed between the nozzle (Figure 7a) and the plasma chamber wall at the second 5-kV ETC firing, which had an identical electrode-nozzle liner setup as the first shot. The pressure leaked between the O-ring sealing area at the nozzle sides and the vessel's wall; an area damaged during the previous shot. This pressure displaced the nozzle and E-glass liner away from the vessel's wall, breaking the electrical contact between the copper washer at the front
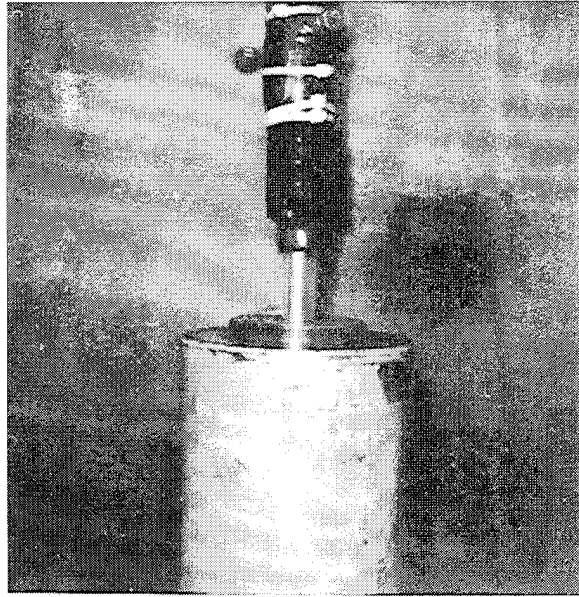
17

Figure 9. PFN to chamber connector.

side of the nozzle and the vessel's wall (ground). A higher resistance path was then created and, consequently, a high energy arc occurred, bonding the nozzle sides to the already damaged vessel's chamber wall. Minor metallic deposits at the nozzle sides were noticed with previous PFN ETC firings at lower energy (13 kJ) and lower input voltages (3 kV), even when the nozzle was in full contact with the vessel's wall. The full mechanism of this phenomenon is not yet completely understood and is still being studied.

4.3 Third ETC Firing. For the third 5-kV ETC firing, the O-ring previously used at the nozzle's wider section (Figure 7a) was installed at the thinner top part of the nozzle (Figure 10), as the chamber walls at the previous location were badly eroded by the arc-welding. The O-ring function was to seal the plasma chamber from combustion gases and to keep the heat loss to about 10% as it sealed the E-glass liner exterior walls from reacting with the propellant combustion gases. An E-glass liner of reduced OD was fitted inside a hollow 0.635-cm wall thick steel liner of the same length (7.52 cm). This assembly (Figure 10) was intended to push the nozzle base against the vessel's chamber wall to eliminate the pressure that was breaking the lower copper resistive path as the E-glass was compressed. The plotted resistance at the load (Figure 11) demonstrates that no shorts occurred. Load current and voltage are shown in Figure 12; power and energy in Figure 13.
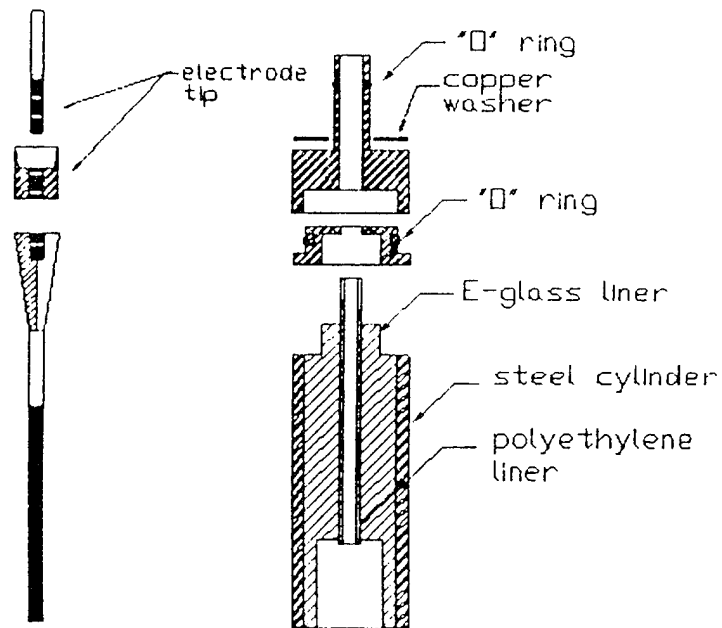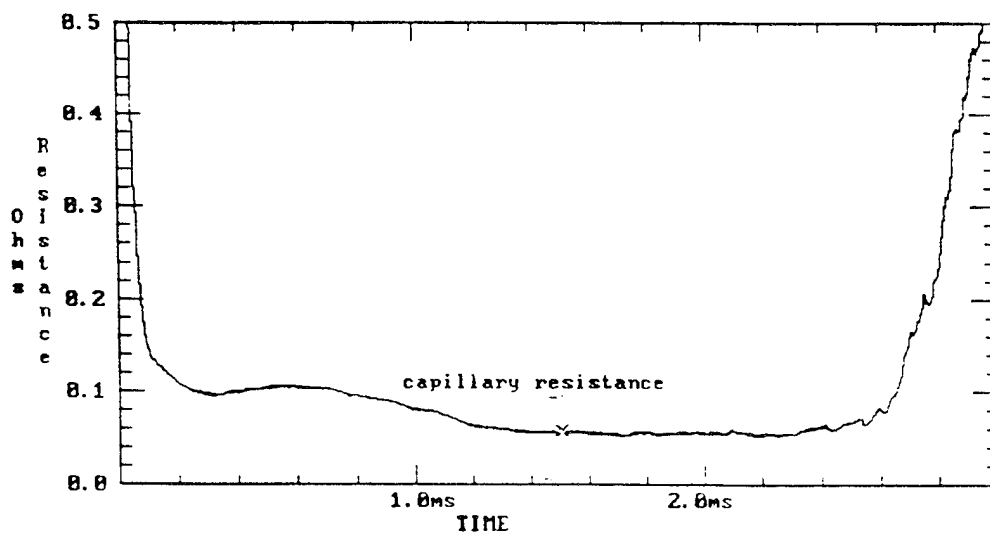
18

Figure 10. Plasma assembly, model 2, schematic.

Figure 11. Capillary resistance, shot 3.
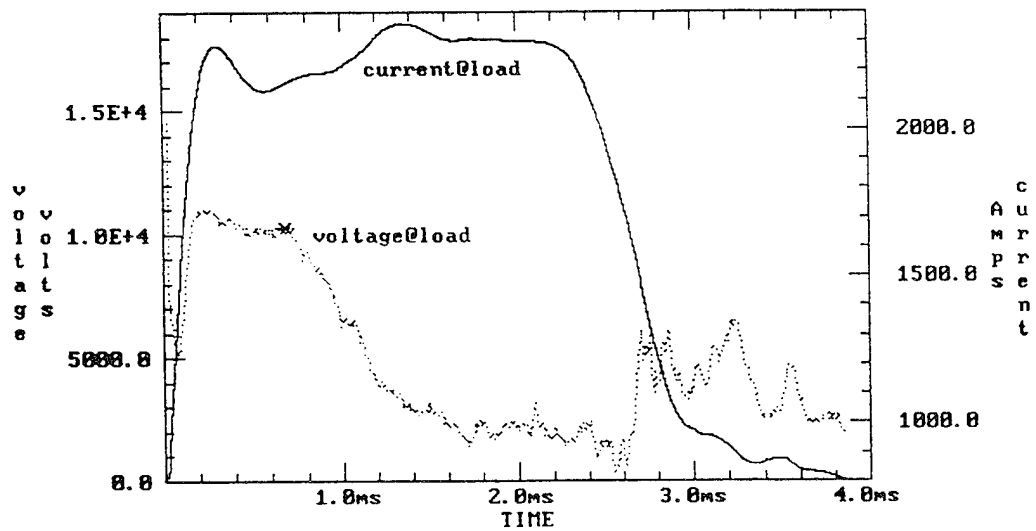
19

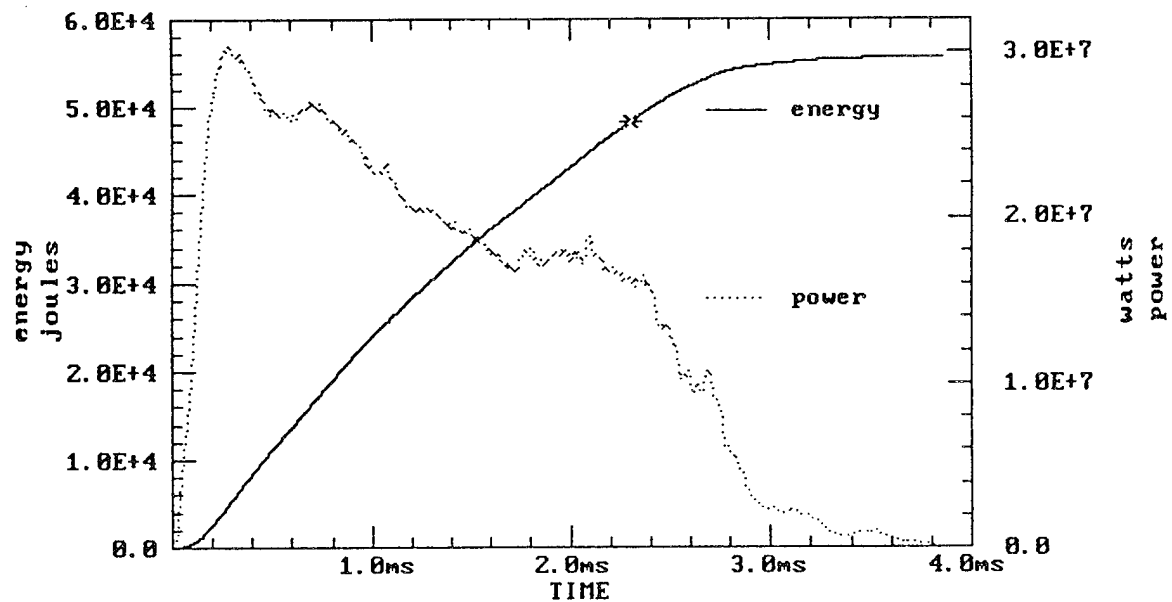Figure 12. <u>Load C and V, shot 3</u>.

Figure 13. <u>Load P and E, shot 3</u>.

4.4 Fourth ETC Firing. Finally, a third model liner and nozzle assembly (Figures 14 and 15) were designed. The erosion nozzle was now completely embedded in the liner. The only surface of this assembly exposed to the chamber wall is its front area, which is substantially less than before. Electrical parameters at the load are shown in Figures 16, 17, and 18.

This fourth firing showed no metallic deposits at the nozzle, which was manufactured as one piece without a tight O-ring fit securing both sections (Figure 7a). The melted electrode tip metal escaped through the nonsealed area between the erosion nozzle and the E-glass liner and into the plasma chamber. It was concluded that the metallic products were forced by the propellant pressure on the sides of the chamber head retaining cap, which holds the sealing elements in place (Figure 7a and 7b). This suggests that the plasma metallic products are forced to flow backwards by the combustion gases outside and around the E-glass liner. This fact also suggests that the electrode insulation damage that caused the short on the first ETC firing was due to plasma metallic products flowing backwards inside the polyethylene liner.

5. CONCLUSIONS

5.1 Achievements. The modified PFN performed as expected, extending the pulse to the desired 2.4-ms length. The output current, voltage, power, and energy verifies that minimal coupling if any, occurs between the inductors, proving that the assembly of the coils in the confined area worked as planned.

Pressure-time data (Oberle et al. 1994) from ETC closed chamber firings indicate maximum pressures significantly lower than expected. A number of reasons have been proposed to explain these results. It is possible that, due to the very high plasma temperature, radiative heating of the pressure transducer element may be taking place. For conventional closed chamber firings, a grease is used to inhibit convective heat transfer to the gage. However, the grease may be transparent to the radiation from the plasma that is nearly 100 times that of the propellant flame (White et al. 1994). Future firings will include techniques to reduce this potential radiative heating of the gage.

ETC testing in a closed chamber has demonstrated a more severe problem with metallic erosion products than for gun firings. The combustion chamber showed absence of metallic deposits created by
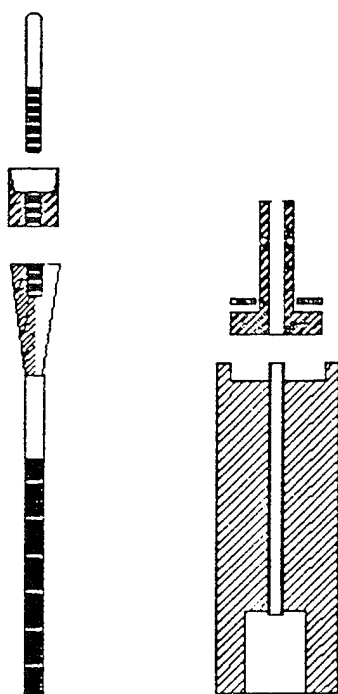
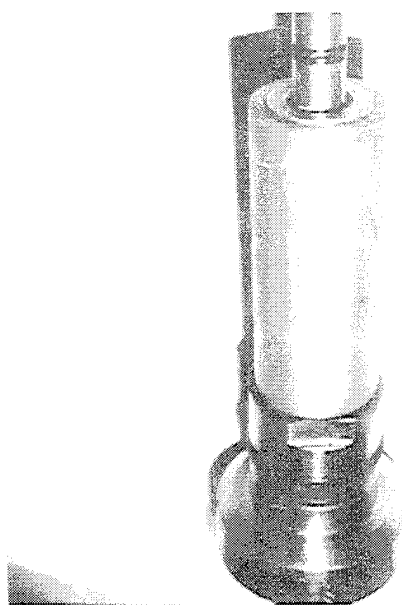Figure 14. Plasma assembly, model 3, schematic.

Figure 15. Model 3, photograph.

22
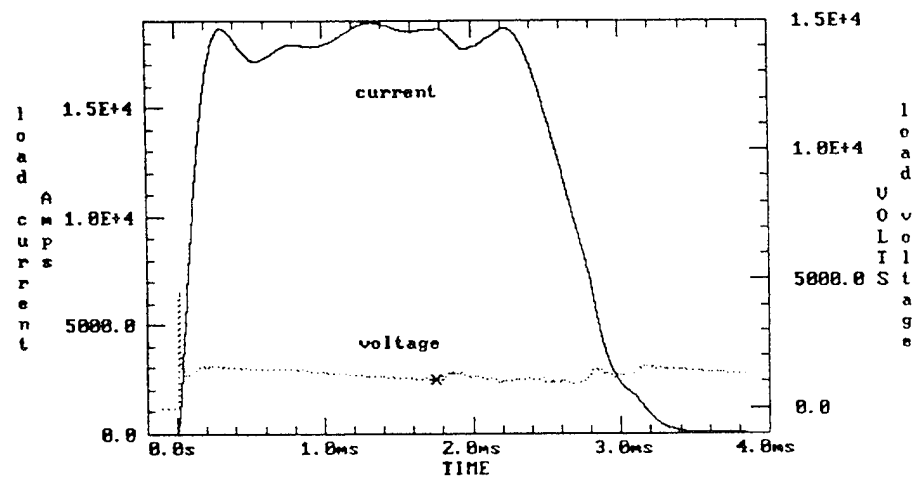
Figure 16. Load C and V, shot 4.
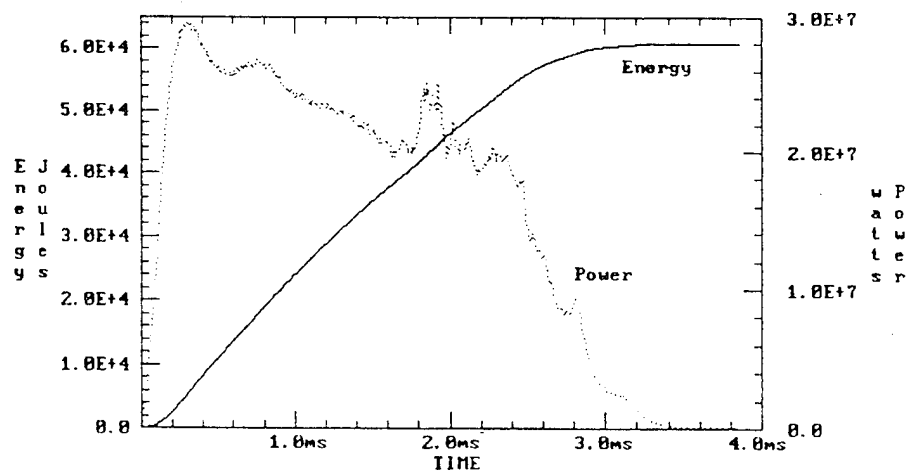
Figure 17. Load P and E, shot 4.

23
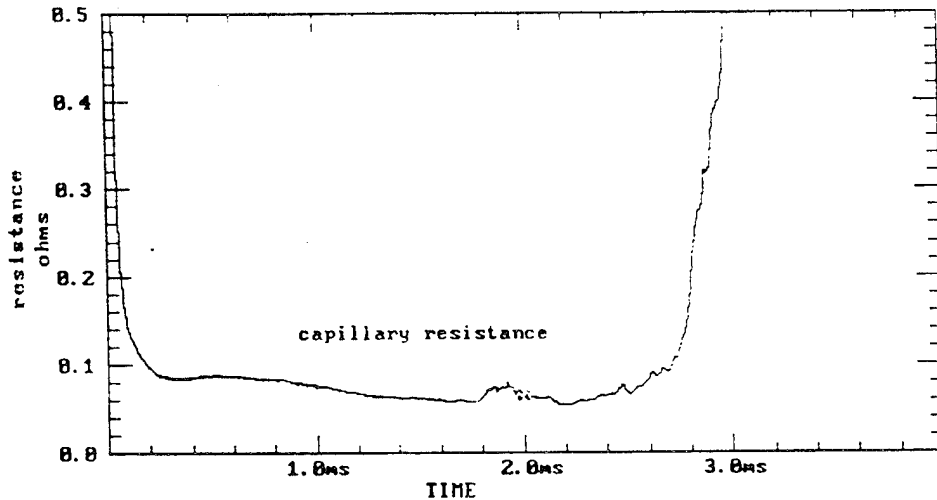
Figure 18. Capillary resistance, shot 4.

the ETC erosion of the electrode and nozzle as they were trapped within the plasma chamber, causing problems with component disassembly. Future plasma generator designs will be directed at preventing these metallic products from escaping the plasma generator's capillary and being deposited on the plasma chamber walls.

The design in Figure 19 shows a nozzle that is threaded at its base and preloads a sealing O-ring as it is screwed into the E-glass liner. Recent tests performed with this type of nozzle at 3-kV charging voltage in a 50-cm^3 vented chamber showed no leaks at the E-glass liner and nozzle joint, or metallic residues bonding any of the plasma generator components onto the plasma chamber.

This result suggests that in all of the designs discussed previously, the polyethylene capillary liner was weakened by the plasma flow into the combustion chamber and by the subsequent pressure created by the ignited propellant flowing backwards into the plasma chamber. This caused the breaking of the capillary liner at the joint between the nozzle base and the E-glass liner.

It is also suspected that during these firings, the preloaded plasma generator assembly, in the process of further compression and expansion during the propellant ignition, experienced detachment at the joint of its nozzle and E-glass liner, contributing to the capillary liner failure.

24
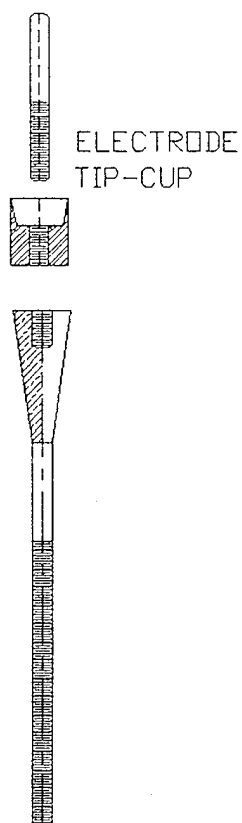
Figure 19a. Electrodes tip and cup assembly.
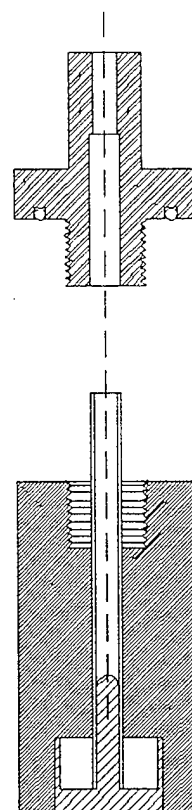
Figure 19b. E-glass liner and erosion nozzle.
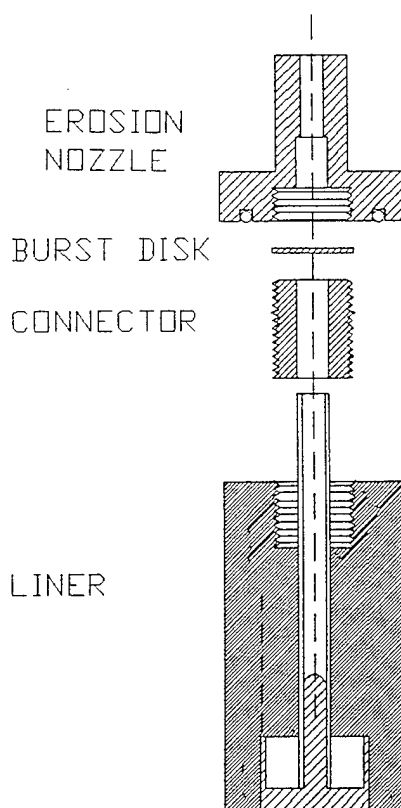
Figure 19c. Plasma delay configuration.

25
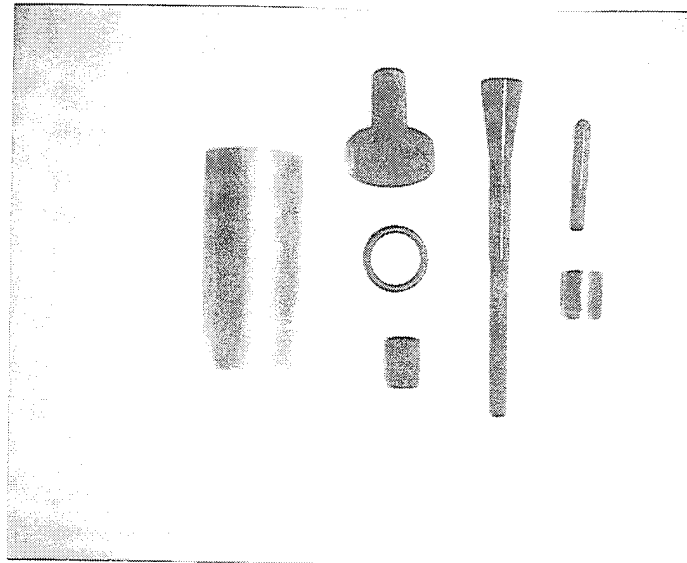
Figure 19d. Model and components.
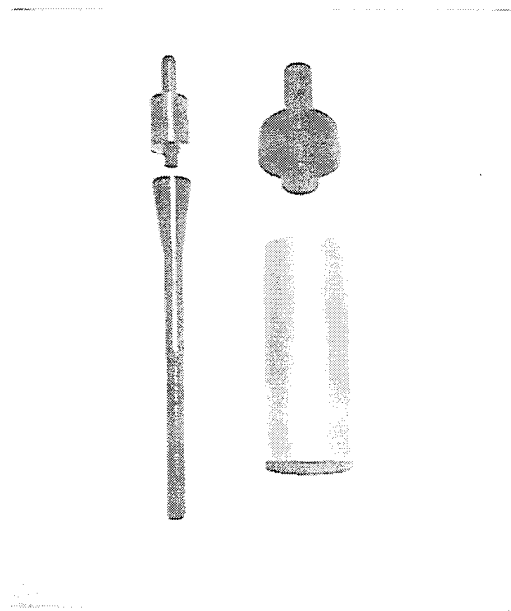
Figure 19e. Assembled model.

5.2 Plans. Future tests will also include a plasma delay device that will allow introduction of the ETC plasma energy later in the ballistic cycle. A new nozzle type (Figure 19) with a burst disk provision to protect the nickel wire path between the anode and cathode during the conventional ignition of the propellant, which occurs prior to the plasma injection, will be used. The energy densities will also be varied to assess the effect of the plasma on propellant burn rates.

26

6. REFERENCES

Bennett, F. D., and J. W. Marvin. Review of Scientific Instruments. Vol. 33, no. 11, pp. 1218–1226, November 1962.

Grover, F. Inductance Calculations, Working Formulas & Tables. Triangle Park, NC: Instrument Society of America, 1982.

Haines, M. G. Proceedings of Phys. Soc., LXXIV, pp. 576–584, 1959.

Haines, M. G. Proceedings of Phys. Soc., vol. 74, pp. 576, 1959.

Katulka, G. L., H. Burden, A. Zielinsky, and K. White. "Electrical Energy Shaping for Ballistic Applications in Electrothermal-Chemical Guns," vol. 1, CPIA Pub. 557, pp. 339–347, November 1990.

Oberle, W. F. "BRLCB: A Closed-Chamber Data Analysis Program, Part I - Theory and User's Manual; Part II - Theory and User's Manual." ARL-TR-36, U.S. Army Research Laboratory, Aberdeen Proving Ground, MD, January 1993.

Oberle, W. F. Private Communication. U.S. Army Research Laboratory, Aberdeen Proving Ground, MD, 1994.

Oberle, W. F., I. Stobie, M. Del Guercio, and K. White. "Analysis of Plasma-Augmented Burn Rates of JA2 Propellant." 31st JANNAF Combustion Subcommittee Meeting, Lockheed Missiles and Space Company, Sunnyvale, CA, October 1994.

Phuong, T. Private Communication. U.S. Army Research Laboratory, Aberdeen Proving Ground, MD, 1994.

White, K. J., W. F. Oberle, A. A. Juhasz, I. C. Stobie, K. Nekula, G. L. Katulka, and S. Driesen. "Combustion Control Requirements in High Loading Density Solid Propellant ETC Gun Firings." 31st JANNAF Combustion Subcommittee Meeting, Lockheed Missiles and Space Company, Sunnyvale, CA, October 1994.

INTENTIONALLY LEFT BLANK.

NO. OF
COPIES   ORGANIZATION

2   ADMINISTRATOR
       ATTN DTIC DDA
       DEFENSE TECHNICAL INFO CTR
       CAMERON STATION
       ALEXANDRIA VA 22304-6145

1   DIRECTOR
       ATTN AMSRL OP SD TA
       US ARMY RESEARCH LAB
       2800 POWDER MILL RD
       ADELPHI MD 20783-1145

3   DIRECTOR
       ATTN AMSRL OP SD TL
       US ARMY RESEARCH LAB
       2800 POWDER MILL RD
       ADELPHI MD 20783-1145

1   DIRECTOR
       ATTN AMSRL OP SD TP
       US ARMY RESEARCH LAB
       2800 POWDER MILL RD
       ADELPHI MD 20783-1145

       ABERDEEN PROVING GROUND

5   DIR USARL
       ATTN AMSRL OP AP L (305)

NO. OF COPIES	ORGANIZATION	NO. OF COPIES	ORGANIZATION
1	OSD SDIO IST ATTN DR LEN CAVENY PENTAGON WASHINGTON DC 20301-7100	1	DIRECTOR ATTN ATCD MA MAJ WILLIAMS HQ TRAC RPD FORT MONROE VA 23651-5143
1	COMMANDER ATTN SMCAR QAH T MR JOHN DOMEN USA ARDEC BLDG 62 NORTH PCNTY ARSNL NJ 07806-5000	1	PRESIDENT US ARMY ARTILLERY BOARD FORT SILL OK 73503
1	COMMANDER ATTN SMCAR AEE BR USA ARDEC MR KEN KLINGAMAN BLDG 1501 PCNTY ARSNL NJ 07806-5000	1	COMMANDANT US ARMY CMD & GEN STAFF COLLEGE FORT LEAVENWORTH KS 66027-5200
1	COMMANDER ATTN SMCAR ASI DR JERRY RUBIN US ARMY ARDEC PCNTY ARSNL NJ 07806-5000	1	COMMANDANT ATTN REV AND TNG LIT DIV US ARMY SPECIAL WARFARE SCHOOL FORT BRAGG NC 28307
1	COMMANDER ATTN ASQNC ELC IS L R MYER CTR USACECOM R&D TECHNICAL LIBRARY FORT MONMOUTH NJ 07703-5301	1	COMMANDER ATTN SMCRA QA HI LIBRARY RADFORD ARMY AMMO PLANT RADFORD VA 24141
5	DIRECTOR ATTN SARWV RD G CARAFANO R THIERRY R HASOENBEIN P VOTIS P ALTO BENET LABORATORIES WATERVLIET NY 12189-4050	1	COMMANDANT ATTN STSF TSM CN US ARMY FIELD ARTILLERY SCHOOL FORT SILL OK 73503-5600
3	COMMANDER ATTN AMSMC IRC G COWAN SMCAR ESM R W FORTUNE R ZASTROW USA AMCCOM ROCK ISLAND IL 61299-7300	4	DEPUTY COMMANDER ATTN SFAE SD HVL S SMITH LTC LEE D LIANOS T ADEN STRATEGIC DEFENSE COMMAND PO BOX 1500 HUNTSVILLE AL 35887-8801
		2	COMMANDER ATTN AMXST MC 3 S LEBEAU C BEITER USA FOREIGN SCIENCE & TECHNLGY CTR 220 SEVENTH ST NE CHARLOTTESVILLE VA 22901
1	COMMANDANT ATTN AVIATION AGENCY US ARMY AVIATION SCHOOL FORT RUCKER AL 36360	1	COMMANDANT ATTN ATSF CO MW B WILLIS USA FIELD ARTILLERY CTR AND SCHOOL FORT SILL OK 73503

NO. OF COPIES	ORGANIZATION
1	NAVAL SEA SYSTEM CMD ATTN CSEA CDR DAMPIER 06KR12 WASHINGTON DC 20362-5101
1	OFFICE OF NAVAL RSRCH ATTN CODE 473 R S MILLER 800 N QUINCY ST ARLINGTON VA 22217
2	COMMANDER ATTN SEA 62R SEA 64 WASHINGTON DC 20362-5101
1	COMMANDER ATTN AIR 954 TECHNICAL LIBRARY NAVAL AIR SYSTEMS COMMAND WASHINGTON DC 20360
1	NAVAL RSRCH LABORATORY ATTN TECHNICAL LIBRARY WASHINGTON DC 20375
2	COMMANDER ATTN J P CONSAGA C GOTZMER NAVAL SURFACE WARFARE CTR SILVER SPRING MD 20902-5000
2	COMMANDER ATTN CODE R 13 K KIM R BERNECKER NAVAL SURFACE WARFARE CTR SILVER SPRING MD 20902-5000
3	COMMANDER ATTN 610 C SMITH 6110J K RICE 6110C S PETERS NAVAL SURFACE WARFARE CTR INDIAN HEAD MD 20640-5035

NO. OF COPIES	ORGANIZATION
6	COMMANDER ATTN CODE G33 T DORAN J COPLEY CODE G30 GUNS & MUNITIONS DIV CODE G301 D WILSON CODE G32 GUNS SYSTEMS DIV CODE E23 TECHNICAL LIBRARY NAVAL SURFACE WARFARE CTR DAHLGREN VA 22448-5000
1	COMMANDER ATTN CODE 270P1 MR ED CHAN NAVAL SURFACE WEAPON CTR 101 STRAUS AV INDIAN HEAD MD 20640
1	COMMANDER ATTN CODE 3120 MR ROBERT RAST NAVAL SURFACE WEAPON CTR 101 STRAUS AV INDIAN HEAD MD 20640
1	COMMANDER ATTN CODE 210P1 MR RON SIMMONS NAVAL SURFACE WEAPON CTR 101 STRAUS AV INDIAN HEAD MD 20640
2	COMMANDER ATTN CODE 6210 SHARON BOYLES NORBERTO ALMEYDA NAVAL SURFACE WEAPON CTR 101 STRAUS AV INDIAN HEAD MD 20640
2	COMMANDER ATTN CODE 3891 MR CHAN PRICE MS ALICE ATWOOD NAVAL AIR WARFARE CTR CHINA LAKE CA 93555
1	COMMANDER ATTN CODE 388 C F PRICE NAVAL WEAPONS CTR INFO SCIENCE DIV CHINA LAKE CA 93555-6001

NO. OF COPIES	ORGANIZATION	NO. OF COPIES	ORGANIZATION
1	OLAC PL TSTL ATTN D SHIPLETT EDWARDS AFB CA 93523-5000	1	THE JOHN HOPKINS UNIV CPIA ATTN T CHRISTIAN 10630 LITTLE PATUXENT PKWY SUITE 202 COLUMBIA MD 21044-3200
10	CENTRAL INTELLIGENCE AGENCY OFC OF CENTRAL REF DISSEMINATION BR RM GE 47 HQS WASHINGTON DC 20502	2	PENNS STATE UNIV ATTN JEFF BROWN DEPT OF MECH ENGRG 312 MECH ENGRG BLDG UNIVERSITY PARK PA 16802
1	CENTRAL INTELLIGENCE AGENCY ATTN JOSEPH E BACKOFEN ROOM 5F22 HQS WASHINGTON DC 20505	1	NCSU ATTN JOHN G GILLIGAN BOX 7909 1110 BURLINGTON ENGRG LABS RALEIGH NC 27695-7909
5	DIRECTOR ATTN T HITCHCOCK R WOODFIN D BENSON S KEMPKA R BEASLEY SANDIA NATL LABS ADVANCED PROJECTS DIV 14 ORGANIZATION 9123 ALBUQUERQUE NM 87185	2	INSTITUTE FOR ADVANCED STUDIES ATTN DR H FAIR DR T KIEHNE 4030 2 WEST BAKER LANE AUSTIN TX 78759-5329
		1	SRI INTERNATIONAL ATTN TECHNICAL LIBRARY PROPULSION SCIENCES DIV 333 RAVENSWOOD AV MENLO PARK CA 94025
2	DIRECTOR ATTN B KASWHIA H DAVIS LOS ALAMOS NATIONAL LAB LOS ALAMOS NM 87545	1	SPARTA ATTN DR MICHAEL HOLLAND 9455 TOWNE CENTER DR SAN DIEGO CA 92121-1964
1	DIRECTOR ATTN M S L 355 A BUCKINGHAM LAWRENCE LIVERMORE NATL LAB PO BOX 808 LIVERMORE CA 94550	5	FMC CORPORATION ATTN MR G JOHNSON MR M SEALE DR A GIOVANETTI MR J DYVIK DR D COOK 4800 E RIVER RD MINNEAPOLIS MN 55421-1498
2	DIRECTOR ATTN R ARMSTRONG S VOSEN SANDIA NATL LABS COMBUSTION RSRCH FACILITY DIV 8357 LIVERMORE CA 94551-0469	2	HERCULES INC ATTN D A WORRELL EDWARD SANFORD RADFORD ARMY AMMO PLANT MGR MANUFACTURING ENGRG DEPT PO BOX 1 RADFORD VA 24141
1	UNIV OF ILLINOIS ATTN PROF HERMAN KRIER 144 MEB DEPT OF MECH INDUST ENGR 1206 N GREEN ST URBANA IL 61801		

32

NO. OF COPIES	ORGANIZATION	NO. OF COPIES	ORGANIZATION
1	HERCULES INC ATTN DR RICHARD CARTWRIGHT 100 HOWARD BLVD KENVIL NJ 07847	2	PRINCETON COMBUSTION RSRCH LABS INC ATTN M SUMMERFIELD M MESSINA PRINCETON CORPORATE PLAZA 11 DEERPARK DRIVE BLDG IV SUITE 119 MONMOUTH JUNCTION NJ 08852
3	GT DEVICES ATTN DR S GOLDSTEIN DR R J GREIG DR N WINSOR 5705A GEN WASHINGTON DR ALEXANDRIA VA 22312	2	SCIENCE APPLICATIONS INC ATTN J BATTEH L THORNHILL 1519 JOHNSON FERRY RD SUITE 300 MARIETTA GA 30062-6438
3	GENERAL DYNAMICS LAND SYSTEMS ATTN DR B VANDEUSEN MR F LUNSFORD DR M WEIDNER PO BOX 2074 WARREN MI 48090-2074	1	ELI FREEDMAN & ASSOCIATES ATTN E FREEDMAN 2411 DIANA RD BALTIMORE MD 21209
2	ALLIANT TECHSYSTEMS INC ATTN R E TOMPKINS J KENNEDY 7225 NORTHLAND DR BROOKLYN PARK NM 55428	1	ROCKETDYNE ATTN MR OTTO HEINEY MAIL STOP BA26 6633 CANOGA AV CONOGA PARK CA 91304
4	OLIN ORDNANCE ATTN V MCDONALD LIBRARY HUGH MCELROY THOMAS BOURGEOIS DENNIS WORTHINGTON PO BOX 222 ST MARKS FL 32355	1	THIOKOL ATTN DR DAVID DILLEHAY LONGHORN DIV MAIL STOP 703 11 PO BOX 1149 MARSHALL TX 75671
1	PAUL GOUGH ASSOCIATES INC ATTN P S GOUGH 1048 SOUTH ST PORTSMOUTH NJ 03801-5423	1	THIOKOL ATTN DR RODNEY WILLER ELKTON DIV 55 THIOKOL RD ELKTON MD 21922
1	PHYSICS INTERNATL LIBRARY ATTN-H WAYNE WAMPLER PO BOX 5010 SAN LEANDRO CA 94577-0599	1	VERITAY TECHNOLOGY INC ATTN MR E FISHER 4845 MILLERSPORT HIGHWAY E AMHERST NY 14051-0305
2	ROCKWELL INTERNATIONAL ATTN BA08 J E FLANAGAN J GRAY 6633 CANOGA AV CANOGA PARK CA 91304	1	VERITAY TECHNOLOGY INC 4845 MILLERSPORT HWY PO BOX 305 E AMHERST NY 14051-0305

NO. OF COPIES	ORGANIZATION	NO. OF COPIES	ORGANIZATION
1	BATTELLE TWSTIAC 505 KING AVE COLUMBUS OH 43201-2693		ABERDEEN PROVING GROUND
		4	CDR USATC ATTN S WALTON G RICE D LACEY C HERUD
2	CA INSTITUTE OF TECHNLGY ATTN L D STRAND MS 125 224 D ELLIOT JET PROPULSION LAB 4800 OAK GROVE DR PASADENA CA 91109	1	DIR USAHEL ATTN J WEISZ
1	GENERAL ELECTRIC CO ATTN DR J MANDZY DEFENSE SYSTEMS DIV MAIL DROP 43 220 100 PLASTICS AV PITTSFIELD MA 01201	39	DIR USARL ATTN AMSRL WT P INGO W MAY AMSRL WT PA AVI BIRK TERENCE COFFEE MIGUEL DEL GUERCIO 3 CP JAMES DE SPIRITO DAWN GORDNER ARPAD JUHASZ
2	SAIC ATTN MR N SINHA DR S DASH 501 OFFICE CENTER DR FORT WASHINGTON PA 19034-3211		JOHN KNAPTON CHARLES LEVERITT MICHAEL MCQUAID KEVIN NEKULA WILLIAM OBERLE SHARON RICHARDSON IRVIN STOBIE
1	STATE UNIV OF NY ATTN DR W J SARGEANT DEPT OF ELECTRICAL ENGRG BONNER HALL RM 312 BUFFALO NY 14260		PHUONG TRAN KEVIN WHITE GLORIA WREN AMSRL WT PB EDWARD SCHMIDT AMSRL WT PC RONALD ANDERSON RICHARD BEYER
1	SCIENCE APPLCTN INTERNATL CORP ATTN DR GEORGE CHRYSSAMELLIS 8400 NORMANDELE BLVD SUITE 939 MINNEAPOLIS MN 55437		JOSEPH HEIMERL ANTHONY KOTLAR AMSRL WT PD BRUCE BURNS AMSRL WT PE ANDREW BRANT LANG MANN CHANG JOSEPH COLBURN
1	SANDIA NATL LABS ATTN MR MARK GRUBELICH DIV 2515 PO BOX 5800 ALBUQUERQUE NM 87185		PAUL CONROY ALBERT HORST GEORGE KELLER DOUGLAS KOOKER DAVID KRUCZYNSKY ROBERT LIEB THOMAS MINOR
1	IMI SERVICES USA ATTN MR G RASHBA 2 WISCONSIN CIRCLE SUITE 420 CHEVY CHASE MD 20815		MICHAEL NUSCA FREDERICK ROBBINS TODD ROSENBERGER AMSRL WT T WALTER F MORRISON

34

USER EVALUATION SHEET/CHANGE OF ADDRESS

This Laboratory undertakes a continuing effort to improve the quality of the reports it publishes. Your comments/answers to the items/questions below will aid us in our efforts.

1. ARL Report Number __ARL-MR-261_____ Date of Report __September 1995_____

2. Date Report Received _____

3. Does this report satisfy a need? (Comment on purpose, related project, or other area of interest for which the report will be used.) _____

_____

_____

4. Specifically, how is the report being used? (Information source, design data, procedure, source of ideas, etc.)

_____

_____

_____

5. Has the information in this report led to any quantitative savings as far as man-hours or dollars saved, operating costs avoided, or efficiencies achieved, etc? If so, please elaborate. _____

_____

_____

6. General Comments. What do you think should be changed to improve future reports? (Indicate changes to organization, technical content, format, etc.) _____

_____

_____

_____

_____
Organization
_____
CURRENT   Name
ADDRESS   _____
                 Street or P.O. Box No.
                 _____
                 City, State, Zip Code

7. If indicating a Change of Address or Address Correction, please provide the Current or Correct address above and the Old or Incorrect address below.

_____
Organization
_____
OLD   Name
ADDRESS   _____
                 Street or P.O. Box No.
                 _____
                 City, State, Zip Code

(Remove this sheet, fold as indicated, tape closed, and mail.)
(DO NOT STAPLE)